Available online at www.sciencedirect.com

ScienceDirect

Geochimica et Cosmochimica Acta 244 (2019) 403–415

Geochimica et Cosmochimica Acta

www.elsevier.com/locate/gca

Vanadium isotope composition of seawater

Fei Wu [a,*], Jeremy D. Owens [a], Tianyi Huang [b,c,d], Adam Sarafian [b,c,e,f], Kuo-Fang Huang [g], Indra S. Sen [h], Tristan J. Horner [c,d], Jurek Blusztajn [c,e], Peter Morton [a], Sune G. Nielsen [c,e]

[a] *Department of Earth, Ocean and Atmospheric Science|National High Magnetic Field Laboratory, Florida State University, Tallahassee, FL 32306, USA*

[b] *Department of Earth, Atmospheric, and Planetary Sciences, Massachusetts Institute of Technology, Cambridge, MA, USA*

[c] *NIRVANA Laboratories, Woods Hole Oceanographic Institution, Woods Hole, MA, USA*

[d] *Department of Marine Chemistry and Geochemistry, Woods Hole Oceanographic Institution, Woods Hole, MA 02543-1050, USA*

[e] *Department of Geology and Geophysics, Woods Hole Oceanographic Institution, Woods Hole, MA, USA*

[f] *Science and Technology Division, Corning Incorporated, Corning, NY 14831, USA*

[g] *Institute of Earth Sciences, Academia Sinica, Taipei, Taiwan*

[h] *Department of Earth Sciences, Indian Institute of Technology Kanpur, UP 208016, India*

Received 30 March 2018; accepted in revised form 7 October 2018; available online 21 October 2018

Abstract

The speciation, burial, and isotopic composition of vanadium (V) in seawater is predicted to be closely coupled to the redox state of the oceans. While the speciation and burial terms are reasonably constrained, the V isotopic composition of seawater has remained elusive owing to significant analytical challenges. To this end, for the first time we have developed and validated a new method to purify V from large volume (≥500 mL) seawater samples that we used to determine the V isotopic composition of seawater. Our method comprises four discrete V-purification steps that exploit ion-exchange chromatography including Nobias chelate and anion exchange resin(s) and measurement by multi-collector inductively-coupled plasma mass spectrometry. Results from several samples with addition of standard V solution with known isotope composition show no isotopic deviation in the chemical and/or analytical procedures and our reproducibility is within typical analytical error for vanadium isotopes measurements. Though V yields were non-quantitative (averaging ≈ 70%) for natural seawater samples, our approach was nonetheless validated with additional experiments. Therein, synthetic seawater solutions of known V isotopic composition with concentration similar to natural seawater were used to confirm that there is limited isotope fractionation during analytical procedures with similar yields. We further tested seawater samples using UV radiation, HNO_3/HCl oxidation, and High-Pressure Asher treatments to ensure there was limited effects from potential non-dissolved phases or variable V speciation such as organic ligand binding of V. All tests except the High-Pressure Asher samples had similar recoveries (i.e. >70%) and all recorded similar isotopic values within error which suggest our method is robust and reliable for V isotopic measurement of seawater. Using our most optimal method, we report V isotope data for several seawater samples from surface and subsurface Atlantic Ocean and deep Pacific Ocean for the first time. Inter-laboratory sample comparison shows that the data was within analysis error (~0.15‰, 2SD). Initial results imply that the deep ocean is isotopically homogeneous with respect to V, and the uptake of V in surface waters appear to cause very limited, if any, isotope fractionation as it is within analytical uncertainties. Thus, our results suggest a reference seawater V isotope composition of $+0.20 \pm 0.15$‰ relative to V isotope standard AA solution. This work analyzes the first V isotope value of seawater which

* Corresponding author.
E-mail address: fwu@fsu.edu (F. Wu).

https://doi.org/10.1016/j.gca.2018.10.010

provides a key foundation for future work to constrain the modern marine V isotope cycle and budget and application for paleoceanographic research.

Keywords: V isotope; Vanadium chemical separation; Multivalence; Isotope analysis; Ocean; Vanadium mass balance

1. INTRODUCTION

Reconstructing the history of Earth's atmospheric and oceanic oxygenation, and reduction-oxidation (redox) states is imperative to illuminate the causal relationship between ocean chemistry and biological evolution (e.g. Lyons et al., 2014). Theoretical investigations and experimental work have shown that isotopes of multi-valence elements can be fractionated during redox reactions (e.g., Ellis et al., 2002; Schauble et al., 2004; Anbar et al., 2005). Thus, isotopic proxies of redox-sensitive elements such as U, Mo, Cr and Tl in marine sedimentary archives can provide unique information of past local and/or global ocean redox conditions (e.g. Arnold et al., 2004; Brennecka et al., 2011; Crowe et al., 2013; Ostrander et al., 2017).

Vanadium (V) is a redox-sensitive element with two, geologically long-lived stable isotopes (^{50}V and ^{51}V) with ^{51}V/^{50}V ratio of ~400. Previous studies have shown that sedimentary V concentrations are coupled to ocean-sediment redox conditions (Algeo and Maynard, 2004; Tribovillard et al., 2006; Owens et al., 2016). Vanadium isotopic measurements, however, have only recently been developed at sufficiently high precision to enable observation of naturally occurring variations (see Nielsen et al., 2011, 2016; Prytulak et al., 2011; Wu et al., 2016). Thus, only a small set of natural samples have been investigated to-date with variations up to 3‰ observed in samples originating from low-temperature environments such as crude oils (Ventura et al., 2015; Gao et al., 2017), marine ferromanganese nodules (Wu et al., 2016), and some V-rich minerals (Schuth et al., 2017). These variations are consistent with a recent theoretical calculation study that showed significant V isotope fractionations are likely between V species with different valences and chemical binding environments (Wu et al., 2015). This suggests that V isotopes could be significantly fractionated in Earth's surficial environments due to valence state changes caused by redox reactions and/or mineral adsorption, which are likely the main processes that control the transportation and segregation of V in solution (Breit and Wanty, 1991).

The speciation of V in seawater is controlled by pH, Eh and ambient V concentrations. In the modern ocean, vanadium behaves as a conservative or near conservative element with concentration varying between ~30 and 40 nmol/kg (~1.5–2.0 μg per L) (Collier, 1984; Jeandel et al., 1987; Shiller and Boyle, 1987; Emerson and Huested, 1991; Morford and Emerson, 1999). The oceanic residence time of V is estimated in the range of ~50–100 kyrs, tens of times longer than seawater mixing time (Emerson and Huested, 1991; Algeo, 2004). Under oxic conditions, V exists as a highly-soluble pentavalent vanadate (e.g. HVO_4^{2-} and $H_2VO_4^-$; Lewan, 1982). The primary sink for vanadate in oxic marine environments is adsorption onto ferro-manganese (Fe-Mn) oxides and clay minerals in pelagic sediments (Elderfield and Schultz, 1996, Morford and Emerson, 1999). Dissolved vanadate tends to be reduced to tetravalent vanadyl (e.g. VO^{2+}, $VO(OH)_3^-$), by organic compounds, which promotes adsorption onto settling particles (Breit and Wanty, 1991). Under strongly reducing conditions, vanadyl can be further reduced to highly insoluble trivalent species (e.g. $V(OH)_3$) through interactions with free sulfide, either in the water column or during early diagenesis (Wanty and Goldhaber, 1992). Due to these redox-dependent solubility changes, the geochemical cycle of V in the global ocean is mainly controlled by local or prevailing environmental redox conditions which influence valance state and thereby burial fluxes of V (e.g., Morford and Emerson, 1999; Algeo and Maynard, 2004). Importantly, V drawdown under reducing conditions does not require the presence of sulfide in the water column (Breit and Wanty, 1991; Morford and Emerson, 1999; Algeo and Maynard, 2004; Huang et al., 2015). It is observed in the low oxygen but non-sulfidic waters off the coast of the Louisiana shelf that has decreased dissolved V concentrations (Shiller and Mao, 1999). This is also supported by observations of paleoclimate events where the global response of V drawdown from seawater occurs prior to widespread expansion of water-column euxinia (Owens et al., 2016; Sahoo et al., 2016).

It is likely that the isotopic mass-balance for V in the ocean is controlled by the proportions of various redox states in the ocean. This is likely due to variable isotope fractionation factors between seawater and sedimentary sinks associated with different depositional redox environments (Wu et al., 2015). Consequently, the V isotope system might be sensitive to changes in ocean redox conditions during initial stages of oxygen loss before an expansion of sulfidic conditions on the seafloor, which likely sets V isotopes apart from other paleo-redox isotopic proxies (e.g. Mo) where sulfide appears to play a key role in driving changes in their marine isotopic budgets (Kendall et al., 2017 and reference therein).

The development of V isotopes to track past changes in marine redox conditions requires a thorough understanding of the modern marine isotopic mass balance. A critical first step relies on measuring the modern V isotope composition of seawater which to-date has not been analyzed. However, several analytical hurdles must be addressed to overcome these challenges. First, the relatively low concentration of V in seawater challenges the analytical capabilities as it requires a large volume per analysis while in a high matrix solution. Second, with only two isotopes, it requires extreme confidence that the chemical separation does not

induce V isotope deviation. Third, numerous polyatomic (e.g. $^{36}Ar^{14}N$, $^{34}S^{16}O$) and isobaric (^{50}Cr and ^{50}Ti) interferences are known to compromise the V mass spectrum during mass spectrometric analysis including sulfur from seawater sulfate. These interferences necessitate optimization of tradeoffs between V^+ ion transmission efficiency and resolving power (e.g. Nielsen et al., 2016). Overcoming these analytical challenges is, however, necessary in order to constrain the full potential of V isotopes to trace the evolution of marine redox conditions.

Here, we develop and validate a method to measure the V isotope composition of seawater. We provide a detailed description of the current most optimal methods for preconcentration and chemical separation. Using this method, we report the first V isotope results for seawater samples from the Atlantic and Pacific Oceans, as well as an international CRMs (Certified Refernce Materials). Our results provide the interpretive framework necessary to construct a first-pass V isotope mass balance for the ocean, thereby laying the foundation for future applications of the V isotope redox proxy.

2. SAMPLES AND METHODS

2.1. Seawater samples

Six seawater samples were anlalyzed in this study, several using multiple methods and replicate analysis. The studied samples include the North Atlantic Surface Seawater (NASS-6) reference material distributed by National Research Council of Canada (NRC - CNRC), three samples from the Bermuda Atlantic Time-series Study (BATS), one from the Gulf of Mexico, and one from the Pacific Ocean. NASS-6 is a seawater reference material collected from surface water at Sandy Cove, Nova Scotia (44°03.1′N, 64°42.2′W) in March 2007. The certified concentrations of some metals, including vanadium, are available from NRC/CNRC (https://www.nrc-cnrc.gc.ca/eng/solutions/advisory/crm/certificates/nass_6.html). Three BATS samples were collected with Go-Flo samplers mounted on a rosette equipped with a CTD instrument on R/V Atlantic Explorer from Bermuda Institute of Ocean Sciences (BIOS), Cruise AE0908 on September 2009 (32°18.5′N 64°31.1′W). These unfiltered BATS samples are sampled at depths of 150 m, 650 m and 750 m and acidified to pH < 2 with concentrated HCl and then stored in acid-washed 10 L polypropylene cubitainers for transporting to the laboratory. Surface seawater (~2–3 m) from the Gulf of Mexico (26°6′N, 85°20′W, here denoted as GoM) was collected in 2015 using a trace metal-clean towed 'fish', filtered during collection at sea using an acid-washed Acropak-200 capsule filter (0.2 μm pore size), and stored unacidified in an acid-washed cubitainer until subsampled for analyses. Samples were then acidified to 0.024 M HCl (ultrahigh purity, distilled) and allowed to sit at least three days before column chemistry. Deepwater from the North Pacific Ocean was collected at 3500 m at Station ALOHA (A Long-term Oligotrophic Habitat Assessment; ~22°45′N, 158°W, here denoted as S9) during the 2002 Intergovernmental Oceanographic Commission (IOC) cruise using trace metal-clean 30-L Go-Flo samplers, filtered shipboard using acid-cleaned 142-mm Nuclepore PCTE filters (0.4 μm pore size), and stored acidified (0.012 M HCl, Optima) in acid-washed 500 ml HDPE bottles since 2002. All acids were trace metal grade (e.g., Aristar) or higher, and all water was purified using a Milli-Q deionization system to ≥18.2 MΩ cm^{-2}.

2.2. Methods

2.2.1. V pre-concentration and purification

Considering that achieving optimal isotope measurement precision requires ≥400 ng of V (e.g., Nielsen et al., 2016), all V pre-concentration methods were optimized for 500 mL sample volumes, which contains roughly 750–1000 ng V. Vanadium purification was subsequently performed at Woods Hole Oceanographic Institution (WHOI) within the Non-traditional Isotope Research on Various Adcanced Novel Applications (NIRVANA) laboratory and at Florida State University (FSU) within the geochemistry group at the National High Magnetic Field Laboratory (NHMFL), with slightly different chemical procedures (Fig. 1). We describe the details of these two methods below.

2.2.1.1. WHOI method. Four columns were used to separate vanadium from matrix elements (Fig. 1a). The first two columns consist of a large quartz column, stem of 10 cm in length and 0.6 cm in diameter, with quartz wool inserted as a porous barrier to retain the resins. The first column pre-concentrates V (and other metals) from the salt matrix of seawater and used 1.5 mL of Nobias PA-1 chelating resin (Hitachi High-Technologies, 45–90 μm mesh size) at pH ~ 6 (Sohrin et al., 2008). The Nobias PA-1 chelating resin has both the ethylenediaminetriacetic and iminodiacetic acid functional groups, making it an excellent chelator of several metals including vanadium (Sohrin et al., 2008). For the chemical procedures described below, prior to adding new or more solution the previous volume was completely discharged. Nobias resin was first activated and cleaned using 3 mL methanol. Then 1 ml of 3 M HNO_3 was added and completely drained prior to another addition of 4.5 mL 3 M HNO_3 (documented as 1 + 4.5 mL hereafter) in sequence and then 1 + 4.5 mL H_2O was added to wash out the acid. Before load on seawater, the resin was preconditioned with 1 + 6 mL of ammonia acetate buffer solution (pH ~ 6), which was made by mixing ammonium hydroxide, acetic acid and de-ionized water. Approximately 250 mL of seawater, which was first adjusted to pH of 6 ± 0.1 using the ammonia acetate buffer solution, was loaded onto the column. Under these conditions trace metals were adsorbed onto the resin while the major seawater salt matrixes (Na, K, Mg, Ca) were eluted. Subsequently, V and other retained metals were then eluted and collected with 1 + 15 mL of 3 M HNO_3. The eluted solution was dried down, and re-dissolved into 0.01 M HCl with 1% (volume/volume) H_2O_2. The Nobias resin was added back to a large container and re-used at least 4 times.

Further purification of V was achieved through exchange columns with AG 1-X8 200–400 mesh anion

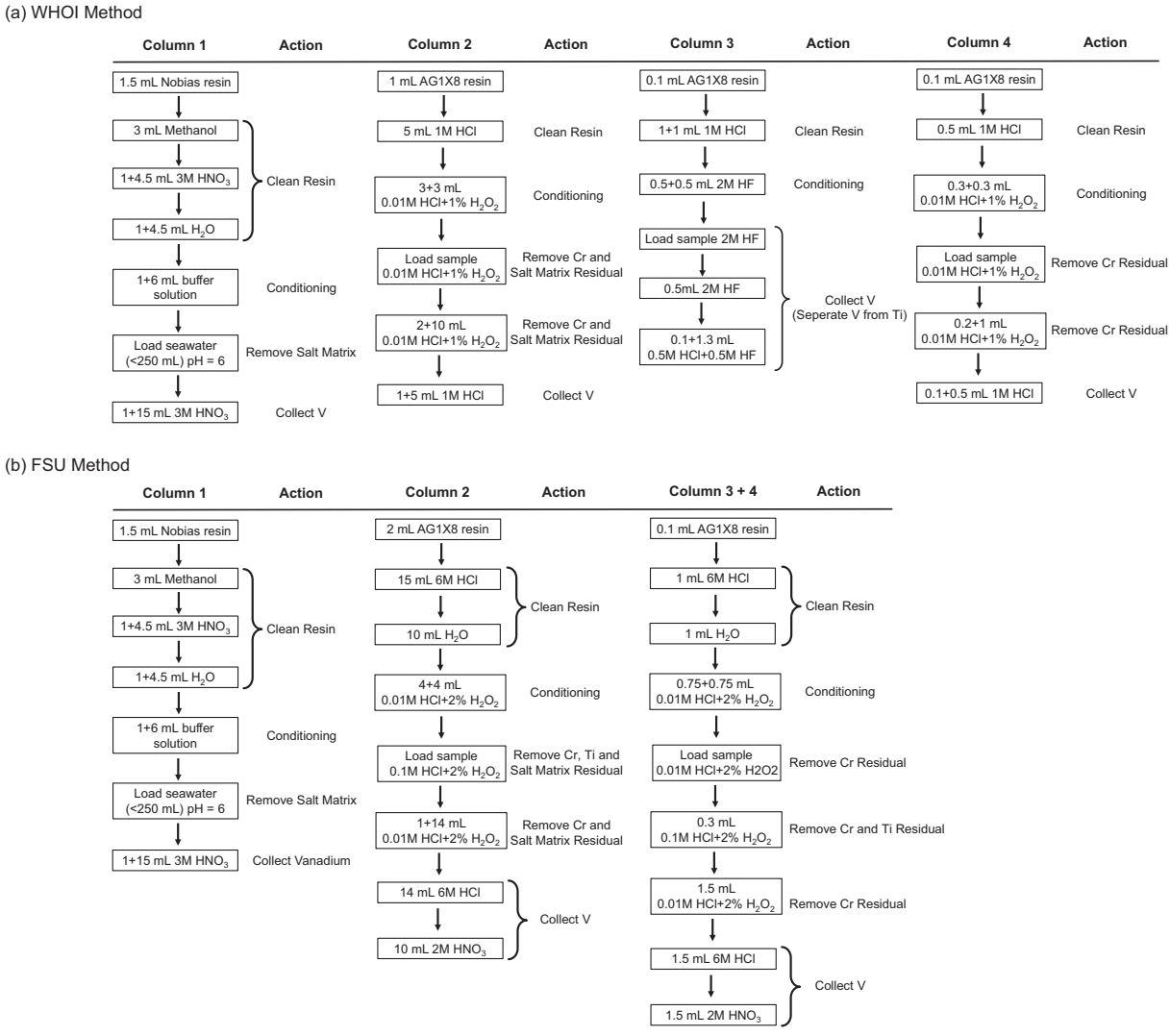

Fig. 1. Summary of the column procedures to separate V from seawater matrices. (a) Analysis based on WHOI method (b) analysis using FSU method.

resins (Bio-Rad Laboratories) largely similar to those described by Nielsen et al. (2011). The anion resins were repeatedly soaked and cleaned with 6 M HCl and H_2O successively for several times before use. In the second column, 1 mL of AG 1-X8 200–400 mesh anion exchange resin was loaded in the quartz columns and cleaned with 5 mL 1 M HCl. Then the resin was pre-conditioned with 3 + 3 mL 0.01 M HCl + 1% (volume/volume) H_2O_2. In this solution pentavalent V forms anionic complexes with H_2O_2 that are strongly adsorbed onto the resin. Because of its rapid dissociation, hydrogen peroxide should be added immediately prior to loading the sample onto the column. After loading the samples onto the resin bed, another 2 + 10 mL 0.01 M HCl + 1% (volume/volume) H_2O_2 was loaded to elute off the residual matrix compounds including Cr. Vanadium was subsequently eluted and collected with 1 + 5 mL 1 M HCl. The AG 1-X8 anion exchange resin was used for only once and throwing away after use. The solution was dried down, and re-dissolved into 0.5 mL 2 M HF.

The final two columns were employed to ensure quantitative removal of residual Ti and Cr. They were mini-columns with 0.1 mL resin volume using AG 1-X8 200–400 mesh resin and follow procedures previously described (Nielsen et al., 2011). In the first mini-column after Makishima et al. (2002), which retains Ti while eluting V, the resin was cleaned and pre-conditioned with 1 + 1 mL of 1 M HCl and 0.5 + 0.5 mL of 2 M HF, respectively. Sample solutions were loaded on to the column, and the eluent was immediately collected. Another 0.5 mL of 2 M HF and then 0.1 + 1.3 mL of 0.5 M HCl + 0.5 M HF were also added and collected together with the sample load. The last mini-column was identical to the second column except that all volumes were scaled down by a factor of 10, which is applied to further eliminate Cr. In between each column procedure, samples were refluxed in aqua regia for at least

four hours to break down minor amounts of organic resin material that had eluted together with V. The final purified V sample was dissolved in 2% (volume/volume) HNO_3 before isotope analysis.

2.2.1.2. FSU method. Four columns were applied to separate vanadium from matrix elements and interferences (Fig. 1b). The first column was identical to that used in the WHOI method. The second column used the same general procedure as the WHOI method, while relied on different column dimensions and resin and reagent volumes. In addition, we found that Ti could also be eluted with Cr if we use 0.1 M HCl + 2% (volume/volume) H_2O_2 rather than 0.01 M HCl + 1% (volume/volume) H_2O_2 for the anion column. Thus, we further modified the anion column step at FSU. The procedure was performed in a pre-cleaned Bio-Rad Poly-Prep chromatography column (9 cm high and 2 mL bed volume) loaded with 2 mL of AG 1-X8 200–400 mesh resin. The AG 1-X8 resin was first cleaned and pre-conditioned using 15 mL of 6 M HCl, 10 mL of H_2O, and 4 + 4 mL of 0.01 M HCl with 2% (volume/volume) H_2O_2, respectively. The sample that had been dissolved in 10 mL of 0.1 M HCl + 2% (volume/volume) H_2O_2 was then loaded on the column. Another 1 + 14 mL of 0.01 M HCl and 2% (volume/volume) H_2O_2 was added to remove residual matrix elements including Cr. The V portion was subsequently eluted and collected with 14 mL of 6 M HCl + 10 mL of 2 M HNO_3. The solution was then dried down, and re-dissolved into 1 mL 0.01 M HCl with 2% (volume/volume) H_2O_2.

Similar mini-columns to those used in the WHOI method with 0.1 mL AG 1-X8 200–400 mesh resin were also used in the FSU method to remove minor amounts of residual Ti and Cr. However, the columns that utilize HF were omitted from the FSU method. For the third column procedure, resin loaded onto the columns were cleaned and pre-conditioned with 1 mL 6 M HCl, 1 mL H_2O, and 0.75 + 0.75 ml 0.01 M HCl with 2% (volume/volume) H_2O_2, respectively. Samples in 1 mL of 0.01 M HCl with 2% (volume/volume) H_2O_2 were then loaded and matrix elements were eluted with 0.3 mL of 0.1 M HCl with 2% (volume/volume) H_2O_2 and 1.5 mL of 0.01 M HCl with 2% (volume/volume) H_2O_2 successively. The additional step using 0.1 M HCl was found to be efficient at removing Ti. The V was subsequently eluted and collected with 1.5 mL of 6 M HCl + 1.5 mL of 2 M HNO_3. The fourth column was a repeat of the third and was employed to ensure complete removal of Cr and Ti. As described for WHOI method, samples were refluxed in aqua regia in between all columns and dissolved in 2% (volume/volume) HNO_3 for isotopic analysis.

2.2.2. Mass spectrometry

Instrument measurements were performed at both WHOI and FSU with similar configurations at both institutions using a Thermo Scientific Neptune Multicollector-Inductively Coupled Plasma-Mass Spectrometer (MC-ICP-MS). Measurements were performed on the flat-topped shoulder on the lower mass side of the overlapping V and molecular interference peaks in medium-resolution mode (resolution $\Delta M/M > 4000$) to resolve all interfering molecular species representing combinations of C, N, O, S, Ar and Cl (such as $^{36}Ar^{14}N^+$, $^{36}Ar^{16}O^+$, and $^{38}Ar^{14}N^+$, see Nielsen et al., 2016; Wu et al., 2016). Jet sample and Ni X-skimmer cones were used to obtain the highest possible V transmission efficiency. In addition, the amplifiers with 10^{10} Ω and 10^{11} Ω resistor were applied to monitor ^{51}V and ^{50}V signal, respectively. We applied dry plasma inlet system with Aridus II desolvator (CETAC Technologies). The typical sensitivity under such configuration was ~150–250 volts/ppm. The configuration requires 400 ng of V for at least one V isotope measurement.

While the chemical purification quantitatively separates Ti and Cr from V, minor amounts of Ti and Cr in solution can still dramatically affect the isotopic value especially for low V concentration measurements. Therefore, analysis of the $^{49}Ti/^{51}V$ and $^{53}Cr/^{51}V$ ratios are needed and should be less than 0.00005 to properly correct for interferences of ^{50}Cr and ^{50}Ti. Here we use the procedure described by Nielsen et al. (2011) and Wu et al. (2016) to correct the raw data for any potential interferences. Briefly, 100 ppb Cr and 100 ppb Ti standard solutions were analyzed before each sequence analysis. These were used to correct for the instrumental mass bias factor (β) for Cr and Ti which are calculated with the assumption of the natural abundances of ^{49}Ti, ^{50}Ti, ^{50}Cr and ^{53}Cr in the standard solutions (de Laeter et al., 2003). The ion beam intensities of ^{50}Ti and ^{50}Cr were then subtracted from the signal mass 50 from the measured ^{49}Ti and ^{53}Cr ion beams for each sample with the calculated β values.

Samples were measured using sample-standard bracketing. All V isotope measurements from different labs mentioned in this study used the aliquots of the Alfa Aesar (AA) V standard primary made and distributed by Nielsen et al. (2011) and Prytulak et al. (2011) as the bracketing solution, and V isotopic data are reported in standard δ notation in per mil relative to AA($\delta^{51}V = ((\,^{51}V/\,^{50}V)_{sample}/(\,^{51}V/\,^{50}V)_{AA} - 1) \times 1000$). The AA V standard solution is defined as $\delta^{51}V = 0‰$ (Nielsen et al., 2011). Each sample analysis consists of 40 cycles of 4.194 s integrations and was bracketed by double measurements of AA solution on each side to obtain an average value and stability of the instrument for the highest quality control. After evaluation of two samples a solution standard, BDH, was measured to ensure the performance and stability of the analysis on the MC-ICP-MS. The in-house isotope BDH standard was a 1000 ppm V standard solution originally bought from BDH Chemicals (Nielsen et al., 2011). Analyses of the BDH standard for this work have an overall average $\delta^{51}V$ of $-1.19 \pm 0.15‰$ (2SD), with average $\delta^{51}V$ of $-1.19 \pm 0.17‰$ (2SD, $n = 96$) run at WHOI and $-1.19 \pm 0.10‰$ (2SD, $n = 55$) run at FSU. The average and uncertainty is in agreement within previously reported values by Nielsen et al. (2011) ($-1.19 \pm 0.17‰$, 2SD) that was measured at Oxford and Imperial College, and Wu et al. (2016) ($-1.23 \pm 0.08‰$, 2SD) which was measured at University of Science and Technology of China. Thus these four laboratories with the same

researchers have nearly identical values, showing good inter-laboratory agreement. Sample solutions were run at concentrations of 400–600 ng/mL of V and the concentrations were matched to within 10% of the bracketing standards. All sample measurements were performed with ^{51}V ion beam intensities greater than ~1 nA for optimal measurements (Nielsen et al., 2016).

3. TESTS OF METHOD PERFORMANCE

A successful method for V isotope analysis of seawater must ensure that the final solution after purification must be amenable to precise and accurate V isotopic measurement and faithfully represents the V isotope composition of the seawater. In addition, matrix elements present in sample solutions may significantly reduce the precision and accuracy of isotopic determinations. Thus, we need to verify there is no isotope deviation during chemical purification, such that the measured isotope composition faithfully represents the isotopic composition of V initially present in seawater. Here, several tests were developed to determine the optimized strategy for the purification of V and evaluate the fidelity of the entire chemical purification procedure for seawater samples, as presented below.

3.1. Maximum volume optimization for Nobias resin

Two methods were assessed in this study to determine the optimal procedure for using the Nobias resin to preconcentrate V from seawater prior to anion-exchange chromatography. The first method used a 'bulk extraction' procedure where 1.5 mL of Nobias resin was added to pH 6 buffered seawater and vigorously mixed for about 2 h. The resin and seawater were then filtered using the large quartz columns described in Section 2.2.1. In the second 'column method' test, 1.5 mL Nobias resin was first loaded into the stem of the quartz column, followed by loading of seawater after resin cleaning and pre-conditioning. Samples in both tests were spiked with ~100 μg of AA vanadium solution. In general, we found that the bulk extraction procedure was less efficient in retaining the V than the column method. It is possible that the low recovery using the bulk extraction procedure was due to homogeneous V distribution throughout the resin during the mixing of resin and seawater. Thus, when separating the resin from the large volume of seawater matrix in the quartz columns afterwards, the elution of the seawater matrix could have caused slight downward movement of V in the quartz column, which resulted in a small loss of V (5–10%). As such, we opted for the column method in all subsequent tests and sample processing, though we note that the bulk extraction procedure could likely be modified to obtain similar results.

For the column method, we further performed tests using 1.5 mL of resin with various volumes of seawater spiked with ~100 μg AA V solution to determine the maximum volume of seawater that can be loaded onto the column without losing significant amounts of V. Our tests revealed that ~90% recovery could be achieved with 500 mL of seawater, while using the same amount of resin with 250 mL seawater yielded ~100% recovery. Thus, our work suggests that no more than 250 ml seawater should be loaded onto the column with 1.5 mL Nobias resin in order to ensure near quantitative recovery of V. For a single seawater measurement using 500 mL of sample, it is required that two columns of Nobias resin are employed. Subsequently, the eluted solutions are combined for further chromatography. The Nobias resin can be recycled and used multiple samples. Although we have not ascertained how many uses one batch of resin can withstand, there is no relation to the recovery with the number of times the resin was used.

3.2. Yield optimization tests

3.2.1. Standard addition seawater experiments

Experiments were conducted at WHOI to test the fidelity of the entire chemical purification procedure for seawater samples to ensure the effective removal of all interferences with minimal loss of vanadium. To test this, we added to 250 mL of natural seawater sample between 10 μg and 25 μg of AA standard vanadium solution, then performed the chemical purification with our standard column procedures. Since the total V contained in 250 mL of natural seawater is ~500 ng, the isotope composition of the V recovered should be very close to that of the AA standard solution ($\delta^{51}V = 0$). The average value of spiked samples is $\delta^{51}V = -0.01 \pm 0.08‰$ (2SD, $n = 7$), which is within analytical error of the true value for the AA standard and suggests that there is no detectable V isotope deviation or other isotopic matrix effects associated with the purification method. The average recovery was $96 \pm 6\%$, which indicates that there was minimal loss during the purification procedure. All data are shown in Table 1.

3.2.2. Natural seawater samples

The results of natural seawater samples are shown in Table 2. For an inter-laboratory comparison of WHOI and FSU, we ran a BATS sample from 750 m water depth and NASS-6 with the slightly different chemical procedures (as described in Section 2.2.1). The average $\delta^{51}V$ values of

Table 1
$\delta^{51}V$ data of spiked samples.[a]

Sample no.	$\delta^{51}V$ (‰)	2SD	Recovery	n	Spiked AA (μg)
VSW4-1	0.04	0.09	87	2	25
VSW4-2	−0.02	0.01	94	2	25
VSW4-3	−0.08	0.06	92	2	10
VSW4-4	−0.01	0.19	99	3	25
VSW5-1	−0.01	0.23	99	5	25
VSW5-2	0.02	0.19	105	5	25
VSW5-3	−0.04	0.31	95	5	10
Average	−0.01	0.08			

(n) is the times of repeated measurements of the same solution; 2SD = 2 times the standard deviation of the population of n repeated measurements.

[a] These samples were analyzed at an early stage of the project before we had developed the most optimal mass spectrometric setup for medium resolution MC-ICP-MS. Thus, some of the data are less precise than what the present method is capable of producing.

Table 2
Vanadium isotopic compositions of seawater samples.

Sample site	Sample no.	$\delta^{51}V$ (‰)	2SD	*n*	Split	Recovery	Lab	Notes
BATS 150 m	VSW6-1	0.13	0.16	1	1	76	WHOI	
BATS 650 m	VSW10-1	0.12	0.17	1	1	40[a]	WHOI	Asher
BATS	VSW7-1	0.14	0.24	1		71	WHOI	UV irradiation
750 m	VSW7-2	0.10	0.16	1		69	WHOI	
	VSW7-3	0.13	0.17	1		71	WHOI	
	VSW8-1	0.16	0.17	1		69	WHOI	HNO3/HCl oxidation
	VSW-FSU	0.23	0.01	3		79	FSU	
	Average	**0.18**	**0.11**	**7**	**5**			
NASS-6	NASS-6-1	0.25	0.22	1		73	WHOI	
Surface	NASS-6-2	0.39	0.17	1		64	WHOI	UV irradiation
	NASS-6-3	0.29	0.17	1		68	WHOI	
	NASS-6-4	0.40	0.17	1		67	WHOI	
	NASS-FSU	0.28	0.10	3		75	FSU	
	Average	**0.32**	**0.13**	**7**	**5**			
Gulf of Mexico	GoM-FSU-1	0.25	0.11	3		73	FSU	
Surface	GoM-FSU-2	0.19	0.04	3		75	FSU	
	Average	**0.22**	**0.10**	**6**	**2**			
S9 (Pacific Ocean) 3500 m	S9 3500-FSU	0.24	0.03	3	1	75	FSU	

(*n*) is the times of repeated measurements of the same solution.
Split refers to the number of individual sample measurements made for that sample.
2SD = 2 times the standard deviation. of the population of n repeated measurements. For samples with one analysis, the 2SD denotes the standard deviation of the results of four bracketing AA standard; for samples with multiple analyses, the 2SD denotes the standard deviation of the population of n repeated measurements.
[a] The low yield of HPA-S sample was probably a result of loss during multiple transfer steps between vessels and/or due to small leak during HPA-S run.

the BATS sample are +0.13‰ ($n = 4$) from WHOI and +0.23‰ ($n = 3$) from FSU, and the average $\delta^{51}V$ values of NASS-6 reference seawater are +0.31‰ ($n = 3$) from WHOI and +0.28‰ ($n = 2$) from FSU. These results show that consistent results were obtained from the two laboratories, especially considering that the long-term external reproducibility is ~0.15‰ (2SD). In addition, $\delta^{51}V$ values of the BATS samples from 150 m and 650 m is +0.13‰ ($n = 1$) and +0.12‰ ($n = 1$) from WHOI, respectively, the average $\delta^{51}V$ values of the GoM sample is +0.22‰ ($n = 2$) from FSU, and the average $\delta^{51}V$ values of the S9 sample is +0.24‰ ($n = 3$) from FSU. The uncertainty of the analysis for each sample is either equal to or smaller than the uncertainty of our long-term reproducibility (±0.15‰, 2SD).

The V contents of purified seawater samples were determined by the MC-ICP-MS based on the comparison of the ion beam intensities measured in samples and those of pure V AA standard solution of known concentration. The yield was then calculated based on a comparison of the measured-to-certified V content of the corresponding sample. Where certified V concentrations were unavailable, 'true' V contents were inferred from literature values for nearby samples (e.g., Jeandel et al., 1987, Shiller and Boyle, 1987, and Shiller, 2016 for the Atlantic, Gulf of Mexico, and South Pacific, respectively). Thus, the recovery of V for these seawater samples could be calculated, as shown in Table 2. For all the natural seawater samples, a consistent ~70% recovery was achieved. Thus, there is a systematic difference between the recovery for seawater samples to which AA V solution with at least 10 μg of V had been added (96 ± 6%) and natural seawater samples (73 ± 4%). The low recoveries of natural seawater could potentially induce laboratory isotope fractionation. Thus, we conducted a series of experiments to identify the potential causes of non-quantitative recovery and to test if the loss of V would lead to isotopic fractionation.

3.3. Identification of V loss and isotopic validation tests

Although we obtained ~100% recovery for seawater with V added, the natural samples only yielded ~70%. The low yield of all the natural seawater samples, therefore, cannot be due to general 30% loss of V for the entire procedure as the only difference between the spiked and unspiked samples were their V concentrations. There are two possible means to explain the observed yield differences between spiked and unspiked seawater samples. (1) Previous studies indicated that the distribution of V in seawater is associated with dissolved organic matter, which could form complex dissolved organic ligands with V (e.g. Cheshire et al., 1977; Lewan and Maynard, 1982). It is possible that such organic ligands would preclude the V from adsorbing to the Nobias resin. Presumably, the consistent yield of ~70% would suggest that ~30% of V in natural seawater is bound by organic ligands or otherwise speciated differently than the expected vanadate (Lewan, 1984). (2) Given that our V addition was several orders of magnitude greater than natural samples there could be a consistent loss of ~200–300 ng of V during the entire column chemical

separation procedure that is independent of the amount of V loaded onto the columns. Such a loss would cause lower yields of natural seawater while having a minor effect on the yield for V addition samples because the natural samples had ~750–1000 ng of V processed through the procedure while V addition seawater samples had between 10 and 25 μg. Here, we performed several tests to identify the potential explanation for the low yield of natural samples and recognize any associated isotope fractionation.

In the first set of tests, we collected the matrix solution eluted during the seawater purification process to produce a V-free seawater matrix. This matrix was then spiked with 1 μg of AA, which rendered the V content of this synthetic seawater-like solution close to that of the natural seawater. The synthetic seawater solution was processed through the entire standard V separation procedure. For comparison, we also made a synthetic seawater solution that was spiked with up to 5 μg AA standard V. The details of each synthetic solution and the results are shown in Table 3 and Fig. 2. Most of the samples except two had similarly low yields with ~80% recovery. These results show that there does appear to be a small loss of V during our column procedure of around 200 ng although the tests suggest the loss can be variable (Table 3). In spite of this, none of the losses recorded for these synthetic seawater samples produce an isotopic fractionation. Two of the synthetic samples document a near 100% recovery of V. Importantly, isotopic measurement of all synthetic samples had $\delta^{51}V$ values of -0.01 ± 0.07‰ (2SD, $n = 7$), which is well within the analytical uncertainty of the true value of 0‰.

In the second set of tests, we applied three methods designed to break down any potential dissolved organic carbon (DOC) molecules and likely reduce ligand-bound V pool prior to column procedures. To make certain that no DOC remained, the three methods utilized progressively more aggressive methods to oxidize the DOC.

In the first method we subjected one BATS sample and one NASS-6 reference seawater sample to UV irradiation. This UV-oxidation method is widely applied to destroy the strong organic ligands that chelate trace metals (e.g. Saito and Moffett, 2001; Biller and Bruland, 2012; Noble et al., 2017). Thus, any V associated with organic ligands will be released during UV irradiation. In brief, aliquots of 500 mL were UV-irradiated for 1 h prior to pH adjustment using a Metrohm 705UV, followed by our standard V separation procedure.

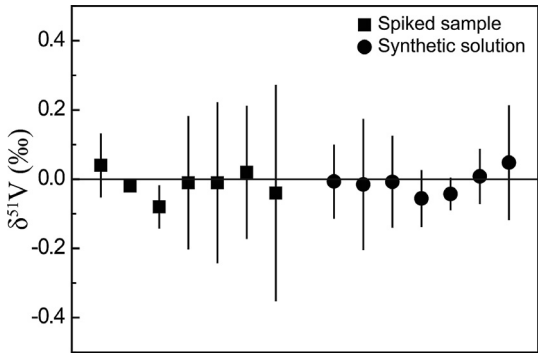

Fig. 2. $\delta^{51}V$ values of standard addition samples and synthetic solutions. Note that the error bar in the figure represents the internal error (2SD) for the individual sample measurement, and the typical external precision of the result is ±0.15‰ (2SD), based on our long-term reproducibility.

In the second method we used aqua regia (HNO_3: HCl = 1:3) to oxidize the DOC. About 220 mL of BATS sample was dried down in a trace metal clean 500 mL Teflon beaker and treated with ~40 ml of aqua regia. The capped beaker was heated at 110 °C on a hotplate for about 14 h, then dried down and re-dissolved into 100 mL ~ 0.01 M HCl, which was ready for pH adjustment and column procedure.

The third method utilized an Anton Paar HPA-S High Pressure Asher system (indicated as HPA-S below). It is a wet digestion instrument that applies high pressure (105 bars) and elevated temperature (260 °C). We dried down ~230 mL of BATS seawater sample in a clean 500 mL Teflon beaker, and then re-dissolved it in 30 mL of concentrated nitric acid. After being heated at 130 °C on a hotplate overnight, the solution was transferred to precleaned quartz vessels, tightly sealed with Teflon tape and a quartz lid, and reacted in the HPA-S for 1.5 h. The sample was then transferred back into a Teflon beaker, dried down, and re-dissolved into 100 mL ~ 0.01 M HCl, which was then pH adjusted to ~6 for column procedure.

The results of these three tests are all shown in Table 2 and Fig. 3. In all three cases, $\delta^{51}V$ of the oxidized seawater samples are within the error of the previous untreated analysis. The recoveries of all the treated samples were similar or even slightly lower than the untreated samples, except for the HPA-S sample which have quite low yield of 40%.

Table 3
$\delta^{51}V$ data of matrix synthesis solutions.

Matrix solution	Volume (mL)	$\delta^{51}V$ (‰)	2SD	*n*	Recovery	Spiked AA (μg)
BATS	500	−0.01	0.10	3	81	1
NASS-6	250	−0.02	0.19	3	82	1
NASS-6	250	−0.01	0.13	6	80	5
Gulf of Mexico	500	−0.06	0.08	3	98	1
Gulf of Mexico	250	−0.04	0.04	3	101	1
Gulf of Mexico	250	0.01	0.08	3	85	5
S9 (Pacific Ocean)	500	0.05	0.16	3	81	1

(*n*) is the times of repeated measurements of the same solution; 2SD = 2 times the standard deviation of the population of n repeated measurements.

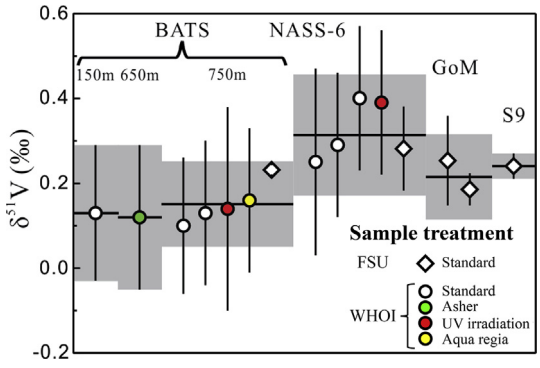

Fig. 3. $\delta^{51}V$ values for seawater samples. Diamond: using the FSU method; Circle: using the WHOI method; white: no additional processing; green: high pressure asher (HPA-S); red: UV irradiation; yellow: Aqua Regia combustion; black line and grey area: average and 2SD error. Note that the error bar in the figure represents the internal error (2SD) for the individual sample measurement, and the typical external precision of the result is ±0.15‰ (2SD), based on our long-term reproducibility. (For interpretation of the references to colour in this figure legend, the reader is referred to the web version of this article.)

The lower yield using the HPA-S was probably a result of loss during multiple transfer steps between vessels and/or potential, but an unlikely cause could be a small leak during the HPA-S run. Additionally, the loss could be due to V adsorption onto the surface of the quartz vessels, although highly unlikely due to the low pH within the vessels.

Overall, the results of the tests indicate that it is unlikely that organic ligand binding of V caused the lower observed yields for the natural seawater samples. More likely, as shown by the synthetic V seawater tests with natural concentration addition of AA, there is a small loss of ~200 ng V associated with the column chemistry V separation procedure. It is currently unclear the exact mechanism of the V loss as it appears to be independent of sample mass loaded onto the column, and this is still an area that requires further work. However, the synthetic V seawater tests also reveal that there is no detectable isotopic fractionation associated with this loss during column chemistry. Hence, we conclude that the overall chemical separation and mass spectrometric method returns precise and accurate V isotope compositions for seawater. However, our tests of the chemical yield suggest that V concentrations in seawater will need to be measured prior to column chemistry with an alternative method due to the loss of ~200–300 ng of V during chemical purification.

4. DISCUSSION

4.1. The V isotope composition of seawater

We report the V isotope results for six seawater samples, five of which are from several water column depths in the Atlantic Ocean and one seawater sample from the deep Pacific Ocean (Table 2). Therein, NASS-6 is from North Atlantic surface water with average $\delta^{51}V$ value of +0.32‰ ($n = 5$), GOM is from the Gulf of Mexico surface water with average $\delta^{51}V$ value of +0.22‰ ($n = 6$), and BATS samples from North Atlantic Ocean at depths of 150 m, 650 m and 750 m, with average $\delta^{51}V$ value of +0.13‰ ($n = 1$), +0.12‰ ($n = 1$) and +0.18‰ ($n = 7$), respectively. Our one Pacific Ocean sample, S9, was collected at a depth of 3500 m, with average $\delta^{51}V = +0.24$‰ ($n = 3$). The typical uncertainty of the result for these samples is ±0.15‰ (2SD), based on our long-term external reproducibility of silicate rocks (Prytulak et al., 2011). Here we plot the $\delta^{51}V$ values of these samples together with vanadium concentration data from the East Pacific Zonal Transect (EPZT) (Fig. 4).

Shallow V concentration minima have been observed in several vertical Pacific surface seawaters profiles (Fig. 4; Collier, 1984; Ho et al., 2017). Additionally, the analysis of V contents in the Atlantic surface waters collected in an open-ocean transect from 22° N to 36° S reveal values between 28 and 35 nmol/kg (Rimskaya-Korsakova et al. 2017), which were similar to or slightly less than deep Atlantic seawater (with average 32–35 nmol/kg, Jeandel et al., 1987; Mlddelburg et al., 1988). Similar surface V concentration minima have also been found in the EPZT (Fig. 4). The V concentration minima in surface seawater is generally attributed to either biological uptake or scavenging onto marine particles/Fe-Mn oxyhydroxides (Collier, 1984; Yeats, 1992). Previous studies have shown that the Gulf of Mexico surface seawater from a nearby station has V contents of ~32 nmol/kg (Shiller and Boyle, 1987), which is similar to the average value of deep Atlantic seawater (32–35 nmol/kg). Our GoM surface seawater samples have a $\delta^{51}V$ value of +0.22‰ ($n = 6$) which is similar to the value of BATS subsurface seawater samples. Given that V concentration minima are only observed in the upper

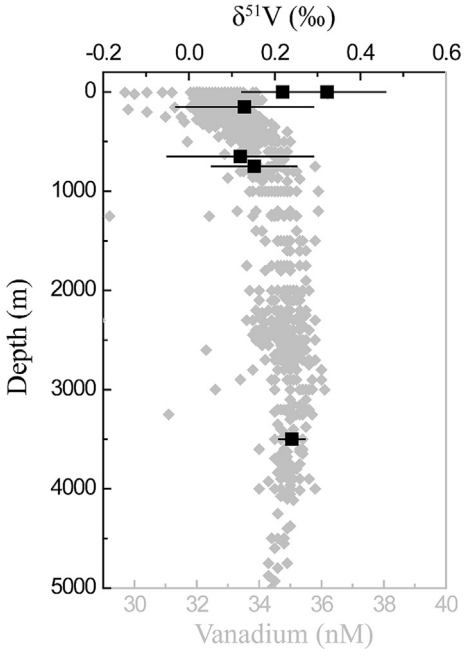

Fig. 4. Average $\delta^{51}V$ values for samples from different depths with V concentration data in Pacific Ocean along the U.S. GEOTRACES East Pacific Zonal Transect (GP16, Shiller, 2016).

~400 m of the water column, it is likely that at least the two deeper BATS samples also have V concentrations comparable to average deep Atlantic seawater. In contrast, the surface seawater sample of NASS-6 shows obvious V depletion relative to the deep seawater with 28 nmol/kg, which is similar to the most depleted V content observed in the Pacific Ocean (Shiller, 2016) and Atlantic Ocean (Rimskaya-Korsakova et al., 2017) surface concentrations. However, the $\delta^{51}V$ value of NASS-6 (+0.32‰, $n = 5$) overlaps with the GoM surface seawater and BATS subsurface seawater samples as all $\delta^{51}V$ are within analytical error. Thus, the uptake of V in surface waters appears to cause limited, if any, isotope fractionation.

Recent analysis for samples collected from 35 hydrographic stations during the U.S. GEOTRACES East Pacific Zonal Transect (GP16) showed that the deep Pacific Ocean has limited variations of dissolved V contents when normalized with average salinity with concentrations of 34.9 ± 1.8 nmol/kg (Fig. 4; Ho et al., 2017). This relationship was even observed in the deep seawater of EPZT below the thermocline which is thought to be influenced by several water masses (Peters et al., 2017). The invariant V concentrations through almost the entire water column are consistent with the relatively long residence time of V (~50–100 kyr) compared to the ocean mixing time of ~1.5 kyr (Collier, 1984; Jeandel et al., 1987; Shiller and Boyle, 1987; Emerson and Huested, 1991; Morford and Emerson, 1999). Thus, it is reasonable to assume that V in the deep ocean is well mixed and likely has a homogeneous V isotope composition. Such a conclusion is in agreements with our observation that the S9 sample from the deep Pacific Ocean has $\delta^{51}V = +0.24‰$ ($n = 5$), which is indistinguishable from that of all the Atlantic seawater data (Fig. 4). Based on our current, albeit limited, data set we suggest that the V isotopic composition of open ocean seawater is homogeneous across all the major ocean basins with a value of $\delta^{51}V = +0.20 \pm 0.15‰$, but more samples from different depth and spatial transects are needed to confirm this hypothesis.

4.2. A first-pass V isotope mass balance for the oceans

Obtaining a V isotope seawater value is a crucial step to decipher global mass balance of the V isotope system. The budget of V in the ocean is mainly controlled by the inputs from various sources versus the accumulation of V into marine sediments (Morford and Emerson, 1999). In the modern, dominantly oxic environment, ocean vanadium behaves as a conservative or near-conservative element, with riverine input as a main source. Thus, the major delivery of dissolved V to the oceans is via riverine input which is mainly driven by weathering of continental crust. In addition, the release of labile V at continental margins associated with riverine particulate material is thought to be another main source of the seawater V, since the depletion of V in continental margin sediments relative to particulate input was observed (Morford and Emerson, 1999; Morford et al., 2005). Hence, all the V inputs into ocean are largely driven by the weathering products of continental material.

The main removal mechanisms of V in the modern ocean is via oxic sediments and hydrothermal sediments (Morford and Emerson, 1999). Assuming steady state is achieved, the influx of V isotopes should be equal to the outflux:

$$\delta_{in} = \delta_{oxic} \times f_{oxic} + \delta_{HT} \times f_{HT} \quad (1)$$

In Eq. (1), δ_{in} represents the V isotope composition of the input, δ_{oxic} represents the V isotope composition of the oxic sink where V(V) is adsorbed by Fe–Mn oxide and deposited in oxic conditions, and δ_{HT} represents the isotopic composition of the V removed by Fe-oxides in the hydrothermal plume. f_{oxic} and f_{HT} represent the proportion of oxic outflux (F_{oxic}) and hydrothermal (F_{HT}) relative to the total flux (F_{total}), i.e., $f_{oxic} = F_{oxic}/F_{total}$, and $f_{HT} = F_{HT}/F_{total}$. Therein,

$$\delta_{in} = \delta_{river} \times f_{river} + \delta_{cont} \times f_{cont} \quad (2)$$

where δ_{river} and f_{river} represent the V isotope composition of riverine input and its proportion relative to the total flux, δ_{cont} and f_{cont} represent the isotope composition of the V released at continental margins and its proportion relative to the total flux. Additional, if we assume that all other input and output fluxes are so small that they can be ignored as a first order assumption (Morford and Emerson, 1999), we have:

$$f_{river} + f_{cont} = f_{oxic} + f_{HT} = 1 \quad (3)$$

With the definition of the isotope fractionation between seawater and sinks, we have:

$$\Delta_{SW-X} = \delta_{SW} - \delta_X \quad (4)$$

where δ_{SW} refers to the V isotopic composition of seawater. Then we can obtain an isotope mass balance of seawater with the combination of the Eqs. (1)–(4) as

$$\delta_{SW} - \delta_{in} = \Delta_{SW-oxic} \times f_{oxic} + \Delta_{SW-HT} \times f_{HT} \quad (5)$$

In oxic waters, vanadate is the dominant species, which is mainly scavenged by Fe and Mn oxides likely through adsorption. For marine sediment, only two ferromanganese nodule standards (NOD-A and NOD-P) have reported $\delta^{51}V$ values currently, i.e. NOD-A, $-1.0 \pm 0.1‰$ (2SD); NOD-P, $-1.7 \pm 0.1‰$ (2SD) (Wu et al., 2016). The large variation of NOD-A and NOD-P is likely due to post-burial diagenesis as NOD-A is thought to be a hydrogenetic, while NOD-P is diagenetic to a hydrogenetic (Bau et al., 2014). Here we use the reported $\delta^{51}V$ value of the one hydrogenetic nodule, NOD-A ($-1.0 \pm 0.1‰$, Wu et al., 2016) as the reference value of oxic modern marine sediment as it is the least altered sample, thus the $\Delta_{SW\text{-}oxic}$ is equal to 1.2‰. Considering the very low accumulation rate of V into oxic sediments (Thomson et al., 1984), we assume $\Delta_{SW\text{-}oxic}$ represents the equilibrium fractionation factor of V during adsorption by Fe-Mn oxyhydroxide.

In hydrothermal system, scavenging of dissolved vanadium from seawater occurs likely by mineral adsorption during the formation of hydrothermal iron oxyhydroxide particles in the plume (e.g. Trocine and Trefry, 1988; German et al., 1991; Feely et al., 1998) which undergo rapid initial uptake into Fe oxyhydroxide phases within the vent

source before being emplaced within the neutrally buoyant plume. Given the rapid kinetics of Fe oxyhydroxide formation, it is plausible that the uptake of V occurred in a semi closed-system, which would suggest that the net fractionation factor for hydrothermal sediments ($\Delta_{SW\text{-}HT}$) should be significantly smaller than that inferred for oxic sediments (e.g. $\Delta_{SW\text{-}oxic} \sim 1.2‰$).

Since the burial flux fractions f_{oxic} and f_{HT} are estimated to be ~0.45 and 0.55, respectively (Morford and Emerson, 1999), we can use Eq. (5) to estimate the currently unknown riverine $\delta^{51}V$ value as $\delta_{in} = -0.6 \pm 0.3‰$. Importantly, the estimated δ_{in} is within the known range of silicate rocks from previous works (Prytulak et al., 2013, 2017; Wu et al., 2016, 2018), implying that our calculation provides reasonable mass balance for the modern ocean V cycle.

5. CONCLUSIONS

We have developed an analytical technique to accurately measure the isotopic composition of V in seawater, for the first time. In this work, we report the first $\delta^{51}V$ seawater values from several ocean basins and water masses with a value of $+0.20 \pm 0.15‰$. Several experiments were conducted to test the fidelity and reliability of our results. Vanadium isotope measurement of seawater samples from surface and subsurface Atlantic Ocean and deep Pacific Ocean indicates that: (1) despite the V concentration minima in surface waters it appears to experience limited fractionations, if any at all, from surface to deep seawater; and (2) V in the deep ocean is well mixed and has a homogeneous V isotope compositions. The observed $\delta^{51}V$ values fit within the range of the known context of marine mass balance V isotope budget.

This new work provides a framework for future V isotope analysis as there are many promising research avenues utilizing V isotopes. As with any new isotope system, there are many underconstrained parameters. Exploring the sedimentary $\delta^{51}V$ is vital to constraining the mass balance cycling of this element especially related to multi-valence state variability (Tribovillard et al., 2006). Concentration work of V suggest this isotope system has the potential to be a powerful proxy for constraining redox changes such as those suggested througout the Precambrian era (e.g. Lyons et al., 2014) and low marine oxygenation environments throughout the Phanerozoic (e.g. Boyer et al., 2011; Gill et al., 2011a, 2011b; Owens et al., 2013, 2016, 2017; Ostrander et al., 2017).

ACKNOWLEDGEMENTS

We would like to acknowledge support from the NSF-OCE 1434785 (to J.D.O. and S.G.N.) and the NASA Exobiology grant NNX16AJ60G (to J.D.O. and S.G.N). This manuscript has benefited from reviews by Morten Andersen, and two anonymous reviewers and editorial handling from Silke Severmann.

REFERENCES

Algeo T. J. (2004) Can marine anoxic events draw down the trace element inventory of seawater? *Geology* **32**, 1057–1060.

Algeo T. J. and Maynard J. B. (2004) Trace-element behavior and redox facies in core shales of Upper Pennsylvanian Kansas-type cyclothems. *Chem. Geol.* **206**, 289–318.

Anbar A. D., Jarzecki A. A. and Spiro T. G. (2005) Theoretical investigation of iron isotope fractionation between $Fe(H_2O)_6^{3+}$ and $Fe(H_2O)_6^{2+}$: Implications for iron stable isotope geochemistry. *Geochim. Cosmochim. Acta* **69**, 825–837.

Arnold G. L., Anbar A. D., Barling J. and Lyons T. W. (2004) Molybdenum isotope evidence for widespread anoxia in mid-proterozoic oceans. *Science* **304**, 87–90.

Bau M., Schmidt K., Koschinsky A., Hein J., Kuhn T. and Usui A. (2014) Discriminating between different genetic types of marine ferro-manganese crusts and nodules based on rare earth elements and yttrium. *Chem. Geol.* **381**, 1–9.

Biller D. V. and Bruland K. W. (2012) Analysis of Mn, Fe Co, Ni, Cu, Zn, Cd, and Pb in seawater using the Nobias-chelate PA1 resin and magnetic sector inductively coupled plasma mass spectrometry (ICP-MS). *Mar. Chem.* **130**, 12–20.

Boyer D. L., Owens J. D., Lyons T. W. and Droser M. L. (2011) Joining forces: Combined biological and geochemical proxies reveal a complex but refined high-resolution palaeo-oxygen history in Devonian epeiric seas. *Palaeogeogr. Palaeoclimatol. Palaeoecol.* **306**, 134–146.

Breit G. N. and Wanty R. B. (1991) Vanadium accumulation in carbonaceous rocks - a review of geochemical controls during deposition and diagenesis. *Chem. Geol.* **91**, 83–97.

Brennecka G. A., Herrmann A. D., Algeo T. J. and Anbar A. D. (2011) Rapid expansion of oceanic anoxia immediately before the end-Permian mass extinction. *Proc. Natl. Acad. Sci.* **108**, 17631–17634.

Cheshire M., Berrow M., Goodman B. and Mundie C. (1977) Metal distribution and nature of some Cu, Mn and V complexes in humic and fulvic acid fractions of soil organic matter. *Geochim. Cosmochim. Acta* **41**, 1131–1138.

Collier R. W. (1984) Particulate and dissolved vanadium in the North Pacific-Ocean. *Nature* **309**, 441–444.

Crowe S. A., Dossing L. N., Beukes N. J., Bau M., Kruger S. J., Frei R. and Canfield D. E. (2013) Atmospheric oxygenation three billion years ago. *Nature* **501**, 535–538.

de Laeter J. R., Böhlke J. K., De Bièvre P., Hidaka H., Peiser H., Rosman K. and Taylor P. (2003) Atomic weights of the elements. Review 2000 (IUPAC Technical Report). *Pure Appl. Chem.* **75**, 683–800.

Elderfield H. and Schultz A. (1996) Mid-ocean ridge hydrothermal fluxes and the chemical composition of the ocean. *Annu. Rev. Earth Pl. Sc.* **24**, 191–224.

Ellis A. S., Johnson T. M. and Bullen T. D. (2002) Chromium isotopes and the fate of hexavalent chromium in the environment. *Science* **295**, 2060–2062.

Emerson S. R. and Huested S. S. (1991) Ocean anoxia and the concentrations of molybdenum and vanadium in seawater. *Mar. Chem.* **34**, 177–196.

Feely R. A., Trefry J. H., Lebon G. T. and German C. R. (1998) The relationship between P/Fe and V/Fe ratios in hydrothermal precipitates and dissolved phosphate in seawater. *Geophys. Res. Lett.* **25**, 2253–2256.

Gao Y., Casey J. F., Bernardo L. M., Yang W. and Bissada K. A. (2017) Vanadium isotope composition of crude oil: effects of source, maturation and biodegradation. *Geol. Soc., London, Spec. Publ.* **468**(SP468), 462.

German C., Campbell A. and Edmond J. (1991) Hydrothermal scavenging at the Mid-Atlantic Ridge: modification of trace element dissolved fluxes. *Earth Planet. Sci. Lett.* **107**, 101–114.

Gill B. C., Lyons T. W. and Jenkyns H. C. (2011a) A global perturbation to the sulfur cycle during the Toarcian Oceanic Anoxic Event. *Earth Planet. Sci. Lett.* **312**, 484–496.

Gill B. C., Lyons T. W., Young S. A., Kump L. R., Knoll A. H. and Saltzman M. R. (2011b) Geochemical evidence for widespread euxinia in the Later Cambrian ocean. *Nature* **469**, 80–83.

Ho P., Lee J.-M., Heller M. I., Lam P. J. and Shiller A. M. (2017) The distribution of dissolved and particulate Mo and V along the U.S. GEOTRACES East Pacific Zonal Transect (GP16): The roles of oxides and biogenic particles in their distributions in the oxygen deficient zone and the hydrothermal plume. *Mar. Chem.*.

Huang J.-H., Huang F., Evans L. and Glasauer S. (2015) Vanadium: Global (bio)geochemistry. *Chem. Geol.* **417**, 68–89.

Jeandel C., Caisso M. and Minster J. F. (1987) Vanadium behaviour in the global ocean and in the Mediterranean Sea. *Mar. Chem.* **21**, 51–74.

Kendall B., Dahl T. W. and Anbar A. D. (2017) The stable isotope geochemistry of molybdenum. *Rev. Mineral. Geochem.* **82**, 683–732.

Lewan M. D. (1984) Factors controlling the proportionality of vanadium to nickel in crude oils. *Geochim. Cosmochim. Acta* **48**, 2231–2238.

Lewan M. D. and Maynard J. B. (1982) Factors controlling enrichment of vanadium and nickel in the bitumen of organic sedimentary rocks. *Geochim. Cosmochim. Acta* **46**, 2547–2560.

Lyons T. W., Reinhard C. T. and Planavsky N. J. (2014) The rise of oxygen in Earth/'s early ocean and atmosphere. *Nature* **506**, 307–315.

Makishima A., Zhu X. K., Belshaw N. S. and O'Nions R. K. (2002) Separation of titanium from silicates for isotopic ratio determination using multiple collector ICP-MS. *J. Anal. At. Spectrom.* **17**, 1290–1294.

Mlddelburg J. J., Hoede D., Van Der Sloot H. A., Van Der Weijden C. H. and Wijkstra J. (1988) Arsenic, antimony and vanadium in the North Atlantic Ocean. *Geochim. Cosmochim. Acta* **52**, 2871–2878.

Morford J., Emerson S., Breckel E. and Kim S. (2005) Diagenesis of oxyanions (V, U, Re, and Mo) in pore waters and sediments from a continental margin. *Geochim. Cosmochim. Acta* **69**, 5021–5032.

Morford J. L. and Emerson S. (1999) The geochemistry of redox sensitive trace metals in sediments. *Geochim. Cosmochim. Acta* **63**, 1735–1750.

Nielsen S. G., Owens J. D. and Horner T. J. (2016) Analysis of high-precision vanadium isotope ratios by medium resolution MC-ICP-MS. *J. Anal. At. Spectrom.* **31**, 531–536.

Nielsen S. G., Prytulak J. and Halliday A. N. (2011) Determination of precise and accurate 51V/50V isotope ratios by MC-ICP-MS, part 1: chemical separation of vanadium and mass spectrometric protocols. *Geostand. Geoanal. Res.* **35**, 293–306.

Noble A. E., Ohnemus D. C., Hawco N. J., Lam P. J. and Saito M. A. (2017) Coastal sources, sinks and strong organic complexation of dissolved cobalt within the US North Atlantic GEOTRACES transect GA03. *Biogeosciences* **14**, 2715.

Ostrander C. M., Owens J. D. and Nielsen S. G. (2017) Constraining the rate of oceanic deoxygenation leading up to a cretaceous oceanic anoxic event (OAE-2:∼ 94 Ma). *Sci. Adv.* **3**, e1701020.

Owens J. D., Gill B. C., Jenkyns H. C., Bates S. M., Severmann S., Kuypers M. M., Woodfine R. G. and Lyons T. W. (2013) Sulfur isotopes track the global extent and dynamics of euxinia during Cretaceous Oceanic Anoxic Event 2. *Proc. Natl. Acad. Sci.* **110**, 18407–18412.

Owens J. D., Nielsen S. G., Horner T. J., Ostrander C. M. and Peterson L. C. (2017) Thallium-isotopic compositions of euxinic sediments as a proxy for global manganese-oxide burial. *Geochim. Cosmochim. Acta*.

Owens J. D., Reinhard C. T., Rohrssen M., Love G. D. and Lyons T. W. (2016) Empirical links between trace metal cycling and marine microbial ecology during a large perturbation to Earth's carbon cycle. *Earth Planet. Sci. Lett.* **449**, 407–417.

Peters B. D., Jenkins W. J., Swift J. H., German C. R., Moffett J. W., Cutter G. A., Brzezinski M. A. and Casciotti K. L. (2017) Water mass analysis of the 2013 US GEOTRACES eastern Pacific zonal transect (GP16). *Mar. Chem.*.

Prytulak J., Nielsen S. G. and Halliday A. N. (2011) Determination of precise and accurate 51V/50V isotope ratios by multi-collector ICP-MS, Part 2: isotopic composition of six reference materials plus the allende chondrite and verification tests. *Geostand. Geoanal. Res.* **35**, 307–318.

Prytulak J., Nielsen S. G., Ionov D. A., Halliday A. N., Harvey J., Kelley K. A., Niu Y. L., Peate D. W., Shimizu K. and Sims K. W. W. (2013) The stable vanadium isotope composition of the mantle and mafic lavas. *Earth Planet. Sci. Lett.* **365**, 177–189.

Prytulak J., Sossi P. A., Halliday A. N., Plank T., Savage P. S. and Woodhead J. D. (2017) Stable vanadium isotopes as a redox proxy in magmatic systems? *Geochem. Perspect. Lett.* **3**, 75–84.

Rimskaya-Korsakova M., Berezhnaya E. and Dubinin A. (2017) Analysis of molybdenum, tungsten, and vanadium in surface water of the Atlantic Ocean using solid phase extraction with 8-hydroxyquinoline and ICP MS determination. *Oceanology* **57**, 530–538.

Sahoo S. K., Planavsky N. J., Jiang G., Kendall B., Owens J. D., Wang X., Shi X., Anbar A. D. and Lyons T. W. (2016) Oceanic oxygenation events in the anoxic Ediacaran ocean. *Geobiology* **14**(5), 457–468.

Saito M. A. and Moffett J. W. (2001) Complexation of cobalt by natural organic ligands in the Sargasso Sea as determined by a new high-sensitivity electrochemical cobalt speciation method suitable for open ocean work. *Mar. Chem.* **75**, 49–68.

Schauble E., Rossman G. R. and Taylor, Jr, H. P. (2004) Theoretical estimates of equilibrium chromium-isotope fractionations. *Chem. Geol.* **205**, 99–114.

Schuth S., Horn I., Brüske A., Wolff P. E. and Weyer S. (2017) First vanadium isotope analyses of V-rich minerals by femtosecond laser ablation and solution-nebulization MC-ICP-MS. *Ore Geol. Rev.* **81**, 1271–1286.

Shiller A. M. and Boyle E. A. (1987) Dissolved vanadium in rivers and estuaries. *Earth Planet. Sci. Lett.* **86**, 214–224.

Shiller A. M. and Mao L. J. (1999) Dissolved vanadium on the Louisiana Shelf: effect of oxygen depletion. *Cont. Shelf Res.* **19**, 1007–1020.

Shiller, Alan (2016) Dissolved copper, nickel, manganese, and vanadium from GeoFISH and bottle samples during the R/V Thomas G. Thompson cruise TN303 from Peru to Tahiti in 2013 (U.S. GEOTRACES EPZT project). Biological and Chemical Oceanography Data Management Office (BCO-DMO). Dataset version 2016-12-20. http://lod.bco-dmo.org/id/dataset/648030.

Sohrin Y., Urushihara S., Nakatsuka S., Kono T., Higo E., Minami T., Norisuye K. and Umetani S. (2008) Multielemental determination of GEOTRACES key trace metals in seawater by ICPMS after preconcentration using an ethylenediaminetriacetic acid chelating resin. *Anal. Chem.* **80**, 6267–6273.

Thomson J., Carpenter M., Colley S., Wilson T., Elderfield H. and Kennedy H. (1984) Metal accumulation rates in northwest Atlantic pelagic sediments. *Geochim. Cosmochim. Acta* **48**, 1935–1948.

Tribovillard N., Algeo T. J., Lyons T. and Riboulleau A. (2006) Trace metals as paleoredox and paleoproductivity proxies: An update. *Chem. Geol.* **232**, 12–32.

Trocine R. P. and Trefry J. H. (1988) Distribution and chemistry of suspended particles from an active hydrothermal vent site on the Mid-Atlantic Ridge at 26 N. *Earth Planet. Sci. Lett.* **88**, 1–15.

Ventura G. T., Gall L., Siebert C., Prytulak J., Szatmari P., Hürlimann M. and Halliday A. N. (2015) The stable isotope composition of vanadium, nickel, and molybdenum in crude oils. *Appl. Geochem.* **59**, 104–117.

Wanty R. B. and Goldhaber M. B. (1992) Thermodynamics and kinetics of reactions involving vanadium in natural systems: Accumulation of vanadium in sedimentary rocks. *Geochim. Cosmochim. Acta* **56**, 1471–1483.

Wu F., Qi Y., Perfit M. R., Gao Y., Langmuir C. H., Wanless V. D., Yu H. and Huang F. (2018) Vanadium isotope compositions of mid-ocean ridge lavas and altered oceanic crust. *Earth Planet. Sci. Lett.* **493**, 128–139.

Wu F., Qi Y., Yu H., Tian S., Hou Z. and Huang F. (2016) Vanadium isotope measurement by MC-ICP-MS. *Chem. Geol.* **421**, 17–25.

Wu F., Qin T., Li X., Liu Y., Huang J.-H., Wu Z. and Huang F. (2015) First-principles investigation of vanadium isotope fractionation in solution and during adsorption. *Earth Planet. Sci. Lett.* **426**, 216–224.

Yeats P. (1992) The distribution of dissolved vanadium in eastern Canadian coastal waters. *Estuar. Coast. Shelf Sci.* **34**, 85–93.

Associate editor: Silke Severmann